Highly sensitive single fibril erosion assay demonstrates mechanochemical switch in native collagen fibrils.

Brendan P. Flynn, Graham E. Tilburey, and Jeffrey W. Ruberti

Department of Mechanical and Industrial Engineering, Northeastern University, Boston, MA, 02115, USA.

j.ruberti@neu.edu

Supplementary Data

1 Glass micro-needle calibration

Glass micro-needles were pulled from solid 1mm borosilicate rods (Sutter Instruments) using a P-97 Browning/Flaming pipette puller (Sutter Instruments). The two pulling profiles were:

	Heat	Pull	Velocity	Time
1	717	50	80	200
2	730	40	100	250

Table S1 Programs used to create glass micro-needles in the pipette puller.

Microneedles were calibrated initially using a cascade of progressively stiffer needle tips. We start with a glass needle stiff enough to calibrate using a laboratory balance and micromanipulator. This calibrated needle is then pressed against a less stiff needle, with the intersection 20 µm from each tip, using micromanipulators and observing at 10-60x. The deflection ratio is used to calculate the stiffness of the less stiff microneedle. This process was repeated with decreasingly stiff microneedles, with many measurements taken at each step, until the desired microneedle stiffness was obtained. The force-deflection stiffness values obtained were linear on force, as was the relative deflection between microneedles.

With stiffness measured for many microneedles of the final desired stiffness (5-60 nN/μm deflection 20μm from the tip), each microneedle was imaged using 60x bright light microscopy and the microneedle geometry was measured using an edge finding routine in Matlab. The microneedle stiffness was then calculated theoretically using the bending equation for a tapered, cantilevered beam:

$$\delta = \int_0^x \int_0^x \frac{M(x)}{Em\, I(x)}\, dxdx = \frac{64}{\pi\, Em} \int_0^x \int_0^x \frac{F\,(L-x)}{D(x)^4}\, dxdx \qquad \text{(S1)}$$

where M, Em, I, and L are the moment, elastic modulus, area moment of inertia, and length. This equation can be rearranged to solve for the deflection stiffness as a function of x, the distance from the tip:

$$\frac{\delta}{F} = \frac{64}{\pi\, Em} \int_0^x \int_0^x \frac{L-x}{D(x)^4}\, dxdx \qquad \text{(S2)}$$

Theoretical stiffness values were typically slightly higher, ~10%, than measured stiffness values. Theoretical calculation uncertainty was calculated to be ~20% for each microneedle, using the direct method, based on the 1.284 μm uncertainty in optical measurement of microneedle geometry.

2 Mounting fibrils to glass micro-needles

Individual collagen fibrils were extracted from a drop of solution in the dish by lifting each end out of solution with a glass micro-needle. A third glass needle, controlled by a custom, manual micromanipulator was used to apply epoxy (Scotch-Weld DP-100, 3M) droplets to the two fibril-micro-needle junctions, 30-50 μm from the needle tips.

3 Mechanical response of collagen fibrils

Mechanically loaded fibrils exhibited an extension without load increase up to a certain point, often termed the “knee,” where load increased linearly with extension.

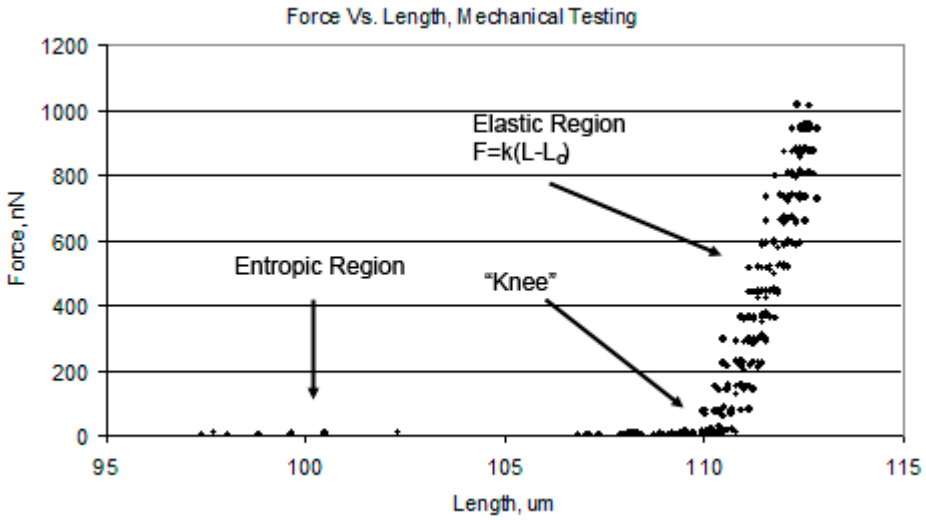

Figure S1: Force vs. Length data for a single collagen fibril with many loading cycles. Each loading cycle showed strong linearity and minimal energy loss/storage with the unloading curve closely following the loading curve.

4 1-D Model

We simplify the degrading collagen fibril to a 1-D radial degradation problem based on the assumption that we have maximal availability of enzyme at the fibril surface. Collagen fibril degradation is limited to surface erosion due to steric obstruction (Okada et al. 1992). A fibril surface, neglecting curvature, contains ~1,712 molecules/μm^2. The native collagen triple helix, a heterotrimer composed of α-chains with Gly-X-Y-repeats, is cleaved by bacterial collagenase A (BC-A) at the X---Gly position in the sequence Pro-X---Gly-Pro-Y (Harper and Kang 1970). Based on bovine type I collagen protein data from NCBI (the National Center for Biotechnology Information) there are ~100 independent BC digestion sites per surface molecule. To calculate the molecular cleavage rate from the radial degradation rate, we consider the ratio of enzyme to available collagen substrate and the time required for enzyme to cover the fibril surface. For a single fibril in solution, the solution is treated as an infinite source, meaning as enzyme molecules bind the fibril the local concentration surrounding the fibril does not change. Considering a rectangular column normal to the fibril surface and the enzyme concentration, 5 μM, a rectangle with height L = 0.4 μm contains the enzyme necessary to cover every surface binding site. Using the diffusion coefficient for bovine serum albumin, a similarly sized globular molecule, of $6x10^{-7}$ cm^2s^{-1} (Raj and Flygare 1974), the diffusion equation solved for time gives,

$t=L^2/4D << 1$ s, where t is the time required for the necessary enzyme molecules to travel the height L of the rectangle.

5 k_{cat}/K_m Calculation

Tzafriri *et al* solve the reaction-diffusion equations for the limiting case of low enzyme and collagen concentrations and find the relationship

$$\frac{d\rho}{dt} \approx -\frac{k_C \kappa E_0}{K_M} \rho^{1/2} \qquad \text{(S3)}$$

where ρ, and E_o represent monomer concentration and initial enzyme concentration respectively, and κ is a size parameter defined as

$$\kappa = \frac{4d_m}{d_f(0)} \rho_o^{1/2} \qquad \text{(S4)}$$

where d_m, $d_f(0)$ and ρ_o are the intermolecular spacing, initial fibril diameter and initial monomer spacing, respectively. Equations S3 and S4 can be combined and rearranged to form

$$\frac{k_C}{K_M} = -\frac{d\rho}{dt}\frac{1}{\kappa E_0 \rho^{1/2}} = -\frac{d\rho}{dt}\frac{d_f(0)}{4d_m \rho_0^{1/2} E_0 \rho^{1/2}} \qquad \text{(S5)}$$

Now, because we have only one fibril, the monomer concentration, ρ, is directly related to fibril diameter by

$$\rho = C \cdot r^2 \qquad \text{(S6)}$$

where C is a constant. Differentiating, S6

$$\frac{d\rho}{dt} = C \cdot 2r \cdot \frac{dr}{dt} \qquad \text{(S7)}$$

Now, substituting Eqs. S6 and S7 into S5, we relate our observable, dr/dt with our desired value

$$\frac{k_C}{K_M} = -\left(C \cdot 2r\frac{dr}{dt}\right)\frac{d_f(0)}{4d_m\left(C \cdot r^2\right)_0^{1/2} E_0 \left(C \cdot r^2\right)^{1/2}} \qquad \text{(S8)}$$

Simplifying, we cancel C and r terms, substituting $2r_0$ for $d_f(0)$

$$\frac{k_C}{K_M} = -\left(2r\frac{dr}{dt}\right)\frac{d_f(0)}{4d_m\left(r^2\right)_0^{1/2}E_0\left(r^2\right)^{1/2}} = -\left(2r\frac{dr}{dt}\right)\frac{2r_0}{4d_m r_0 E_0 r} = -\left(2\frac{dr}{dt}\right)\frac{2}{4d_m E_0}$$

(S9)

Finally, substituting 1.6 for the intermolecular spacing (d_m) we arrive at

$$\frac{k_C}{K_M} = -\frac{dr}{dt}\frac{1}{1.6\cdot E_0} \quad \text{(S10)}$$

6 Mathematical Degradation Model

The failure of low-load fibrils is very interesting, because theoretically, the fibrils should only degrade until they reach a per-monomer load that is completely inhibitive of enzymatic degradation, as was seen for the high-load fibrils. That the low-load fibrils degrade presents a problem for the simple exponential fit of a relationship between applied force per monomer and degradation rate. Zero-load fibrils are not affected by this increase in load, because they are not loaded. High-load fibrils are also not affected by a potential change in force per monomer, because they do not appear to degrade. Mathematical fibril degradation models for low-load fibrils, based on the force-degradation rate results, are presented in figure S1. Note several data fits are used for the force-degradation relationship (single exponential, double exponential, and bi-linear fits) but in each case the fibril approaches a constant diameter at some time point, when the fibril has degraded enough to raise the force per monomer to that of the high-load fibrils, effectively reducing degradation rate to zero.

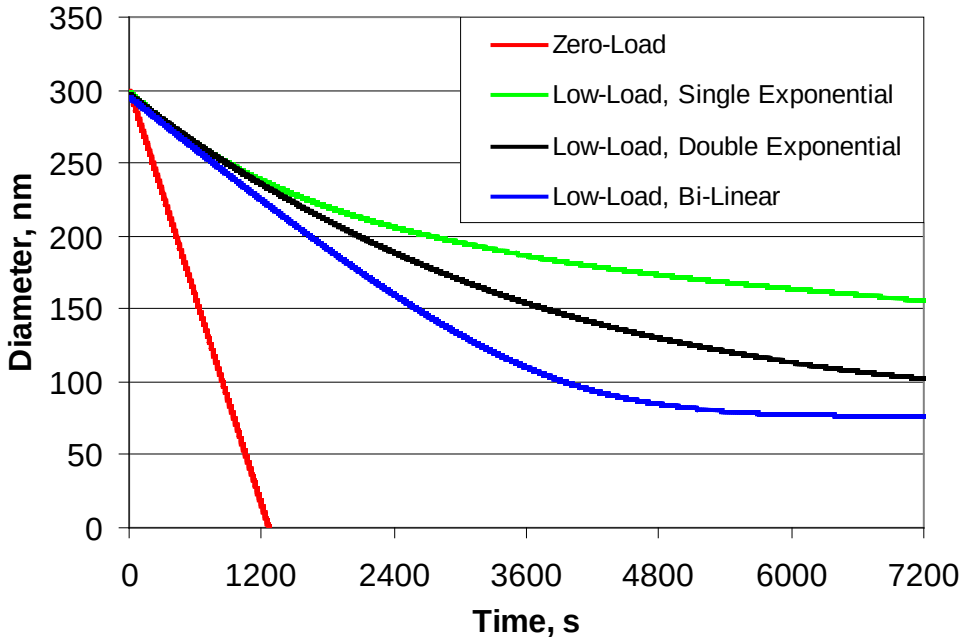

Fig. S1 Theoretical fibril degradation, under low-load, for different force-rate relationships. The zero-load case is provided for comparison. Note that in all low-load cases that the diameter begins to approach a constant value as per-monomer load approaches high-load values and degradation rate approaches zero.

Low-load fibrils typically failed during mechanical probing, where strains reached 20-30% during the final mechanical probe. It is likely that fibrils fail with a significant percentage of the original fibril still un-degraded, because 20-30% strain can be attained with the probe force (~1500nN) for a ~80nm diameter fibril. Interestingly, these values correlate to ~850pN/molecule. We have no explanation for how the low-load fibrils degrade enough to pass through the high-load, zero-degradation regime and continue degrading.

Of additional interest is the potential effect of lost time due to mechanical probing. For zero-load fibrils, 15-20 seconds out of every 300 are spent in a state of load. For low-load fibrils, 10-15 seconds are experience a state of zero-load, followed by 15-20 seconds in a state of higher load. These small intervals may actually have a significant effect on the results, and should be studied/considered in more depth in future investigations.

7 Uncertainty analysis

Force calculations are subject to 14.1% uncertainty in stiffness calibration measurements for each microneedle and a ±214 nm uncertainty in optical bead tracking. For the experiment shown in Fig. 1, this correlates to a force uncertainty of ± 148 nN, or 14%, calculated using the following:

$$Force = TipCalibration * TipDeflection \quad \text{(S11)}$$

$$S_{Force} = \sqrt{\left(\frac{\partial Force}{\partial Calibration}\right)^2 \left(S_{Calibration}\right)^2 + \left(\frac{\partial Force}{\partial Deflection}\right)^2 \left(S_{Deflection}\right)^2} \quad \text{(S12)}$$

$$S_{Force} = \sqrt{\left(Deflection\right)^2 \left(S_{Calibration}\right)^2 + \left(Calibration\right)^2 \left(S_{Deflection}\right)^2} \quad \text{(S13)}$$

$$S_{Force} = \sqrt{\left(18.5\mu m\right)^2 \left(8nN/\mu m\right)^2 + \left(57nN/\mu m\right)^2 \left(0.214\mu m\right)^2} = 148nN \quad \text{(S14)}$$

Forces ranged from 15 ± 2.7 nN (the lowest low-load force) to 1500 ± 212 nN (the highest high-load value), corresponding to 17-14% uncertainty. Note at low forces, and thus low force-deflection values, the uncertainty is dominated by the deflection uncertainty, while at higher forces the uncertainty is dominated by the microneedle calibration uncertainty.

Strain measurements are subject to ± 214 nm uncertainty for each fibril end position, which leads to $\sqrt{2}$*214 nm = 303 nm uncertainty for the length. For the test shown in Fig. 1, these uncertainties in position propagate to a strain uncertainty of ± 0.00385, or 14.4%, calculated using the following:

$$strain = \frac{L_2 - L_1}{L_1} \quad \text{(S15)}$$

$$S_{Strain} = \sqrt{\left(\frac{\partial Stain}{\partial L_1}\right)^2 \left(S_{L_1}\right)^2 + \left(\frac{\partial Stain}{\partial L_2}\right)^2 \left(S_{L_2}\right)^2} \quad \text{(S16)}$$

$$S_{Strain}\sqrt{\left(\frac{-L_2}{L_1^2}\right)^2\left(S_{L_1}\right)^2+\left(\frac{1}{L_1}\right)^2\left(S_{L_2}\right)^2}= \quad \text{(S17)}$$

$$S_{Strain}=\sqrt{\left(\frac{115.7\mu m}{(112.7\mu m)^2}\right)^2(303nm)^2+\left(\frac{1}{112.7\mu m}\right)^2(303nm)^2}=0.00385$$

(S18)

To mitigate gauge length uncertainty, multiple measurements were made. The mechanical testing errors are mitigated by the number of data points taken during each mechanical probe and the linearity of the mechanical response (Fig. 3).

References

Harper E, Kang AH (1970) Studies on the specificity of bacterial collagenase. Biochem Biophys Res Commun 41 (2):482-487. doi:0006-291X(70)90531-0 [pii]

Okada T, Hayashi T, Ikada Y (1992) Degradation of collagen suture in vitro and in vivo. Biomaterials 13:448-454

Raj T, Flygare WH (1974) Diffusion studies of bovine serum albumin by quasielastic light scattering. Biochemistry 13 (16):3336-3340